Characterizing the Lyα forest flux probability distribution function using Legendre polynomials

Agnieszka M. Cieplak* and Anže Slosar†
Brookhaven National Laboratory, Bldg 510, Upton NY 11973, USA
(Dated: September 1, 2016)

The Lyman-α forest is a highly non-linear field with a lot of information available in the data beyond the power spectrum. The flux probability distribution function (PDF) has been used as a successful probe of small-scale physics. In this paper we argue that measuring coefficients of the Legendre polyonomial expansion of the PDF offers several advantages over measuring the binned values as is commonly done. In particular, n-th coefficient can be expressed as a linear combination of the first n moments, allowing these coefficients to be measured in the presence of noise and allowing a clear route for marginalisation over mean flux. Moreover, in the presence of noise, our numerical work shows that a finite number of coefficients are well measured with very sharp transition into noise dominance. This compresses the available information into a small number of well-measured quantities.

arXiv:1608.08808v1 [astro-ph.CO] 31 Aug 2016

I. INTRODUCTION

The Lyα forest, seen as absorption lines of neutral hydrogen along the line-of-sight in quasar spectra, has become a powerful tracer of the underlying matter distribution at high redshift. Its multiple statistics [1], ranging from the evolution of the mean flux with redshift, the transmitted flux probability distribution function (PDF), to the two-point statistics of the power spectrum and correlation function, have been successfully used to probe cosmological parameters (as seen in [2–11] for example).

The flux PDF in particular has been studied since [12] as a way to understand the amplitude of matter fluctuations and the thermal history of the intergalactic medium (IGM). There has been much renewed interest in the flux PDF, since [13] and [14] have found a possible inverted temperature-density relation at $2 < z < 3$ with high resolution, high signal-to-noise (S/N) spectra. This would be in contrast to the theoretical predictions of a positive relation of $T \sim \rho^\gamma$, with $\gamma \sim 1.6$. Most recently, [15] revisited this question with stacked low resolution Sloan Digital Sky Survey (SDSS) spectra and found no such inversion. The flux PDF is therefore an ongoing probe of interest.

However, in addition to being sensitive to the cosmological evolution above, it is also dependent on the pixel noise level, the resolution of the spectra, and the systematic uncertainties in fitting the continuum level [15]. Therefore, the proper treatment of these errors is crucial. [1] first demonstrated the importance of using covariance matrices instead of the pure diagonal error bars in flux PDF measurements. The problem arises with the inversion of this flux PDF covariance matrix, as it is exactly singular [16] due to the normalization integral constraint, making it unnecessarily difficult to calculate noise and correctly fit predicted models [15].

Here we present a different way of encoding the same information, which is arguably systematically cleaner and conceptually nicer.

II. SHIFTED LEGENDRE POLYNOMIAL EXPANSION

The flux field is a three-dimensional field defined through the 3D space

$$F(\mathbf{x}) = e^{-\tau(\mathbf{x})} = \bar{F}\left(1 + \delta_F(\mathbf{x})\right), \tag{1}$$

where $\tau(\mathbf{x})$ is the optical depth due to the Lyα forest, $\bar{F}$ is the mean flux and δ_F are variations around this mean flux. The statistical properties of this field are completely described by the full set of n-correlation functions $\langle F(\mathbf{x}) \cdots F(\mathbf{x}')\rangle$. Usually we measure the 2-point function in real or Fourier space, but much information is present in the field beyond these two. [17] demonstrates that the 1D bispectrum contains at least the same amount of information as the 1D power spectrum. Alternatively, and perhaps somewhat easier routes are via PDFs. After optionally smoothing the field on a certain scale (or the instrument doing it for the observer), the flux PDF $P(F)dF$ is defined as the probability

* acieplak@bnl.gov
† anze@BNL.gov

of the flux being between F and $F+dF$ for a randomly chosen point. This function is uniquely determinable from all possible cumulants (which are in turn given by moments) of the input field and of course also depends on smoothing.

The zeroth moment of the field is unity and the first moment gives the mean flux, which is often unmeasurable in the presence of finite-resolution continuum fitting:

$$\int_0^1 P(F)dF = 1, \tag{2}$$

$$\int_0^1 FP(F)dF = \bar{F}. \tag{3}$$

Traditionally, the flux PDF has been measured in $i = 1 \dots N$ bins of flux, defined by

$$B_i = \int_{(i-1)/N}^{i/N} P(F)dF \tag{4}$$

This gives the constraint $\sum B_i = 1$. While one can write a Bayesian estimator for B_i, it is clear that at least the covariance matrix of the measured B_i is going to be non-positive definite, since the linear combination of $\sum B_i$ modes has zero variance and hence the corresponding eigen-value is zero, making the covariance matrix strictly non-positive definite. In practice, this is mildly annoying but not a show stopper. There are two considerably bigger problems. First, in the presence of noise a simple binning of flux will not give an unbiased estimate of B_i. Second, unless one deals with very high SNR data measured at very high resolution, we can only measure values of δ_F rather than F and hence some marginalisation over $\bar{F}$ is required.

Here we propose an alternative, namely to expand $P(F)$ in terms of shifted Legendre polynomials $L_\ell(x) = \tilde{L}_\ell(2x-1)$, where $\tilde{L}_\ell$ are the standard, unshifted polynomials defined between -1 and $+1$ and $L_\ell(F)$ are the shifted version defined between 0 and 1. Given that this is a complete orthonormal basis, we have:

$$P(F) = \sum_{\ell=0}^{\infty} a_\ell L_\ell(F), \tag{5}$$

$$a_\ell = (2\ell+1)\int_0^1 P(F)L_\ell(F)dF \tag{6}$$

The first few polynomials are given by

$$L_0(F) = 1 \tag{7}$$

$$L_1(F) = 2F - 1 \tag{8}$$

$$L_2(F) = 6F^2 - 6F + 1 \tag{9}$$

$$L_3(F) = 20F^3 - 30F^2 + 12F - 1 \tag{10}$$

$$L_4(F) = 70F^4 - 140F^3 + 90F^2 - 20F + 1 \tag{11}$$

$$\dots \tag{12}$$

Using standard properties of Legendre polynomials, one immediately finds that moments of the flux field are given by

$$M_n = \langle F^n \rangle = \sum_{l=0}^{n} \frac{a_\ell n!^2}{(n-l)!(n+l+1)!}. \tag{13}$$

This is a pretty interesting find. We have made an explicit link between the moments of the distribution and the PDF. More importantly, we have also shown that the first n coefficients a_ℓ are completely determined by the first n moments M_n.

These can be converted to the more observationally relevant quantity: the moments of δ_F, given by $m_n = \langle \delta_F^n \rangle$, with $m_0 = 1$, $m_1 = 0$. Here we have

$$M_n = \bar{F}^n \sum_{k=0}^{n} \binom{n}{k} m_{n-k}. \tag{14}$$

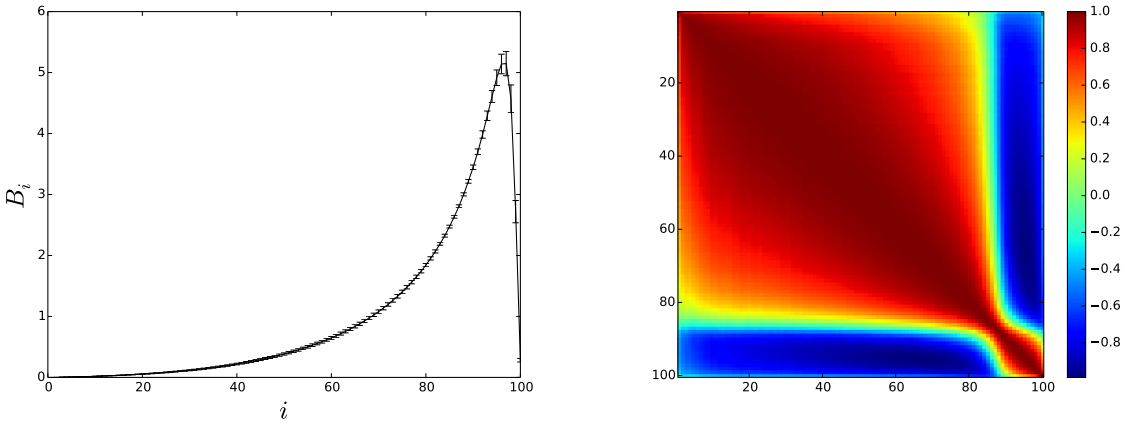

FIG. 1. Values of B_i in left panel with it's covariance matrix in the right panel, at redshift 2, after smoothing the flux field with a smoothing scale of 1 Mpc/h in the line-of-sight direction, with no noise added.

We can therefore express the coefficients of our polynomial expansion a_ℓ combinatorially from observed moments M_n or m_n as

$$a_0 = 1 \tag{15}$$
$$a_1 = 6M_1 - 3 \tag{16}$$
$$a_2 = 30M_2 - 30M_1 + 5 = 30\bar{F}^2 m_2 + 30\bar{F}^2 - 30\bar{F} + 5 \tag{17}$$
$$a_3 = 140M_3 - 210M_2 + 84M_1 - 7 = 140\,\bar{F}^3 m_3 + 420\,\bar{F}^3 m_2 - 210\,\bar{F}^2 m_2 + 140\,\bar{F}^3 - 210\,\bar{F}^2 + 84\,\bar{F} - 7 \tag{18}$$
$$a_4 = 630M_4 - 1260M_3 + 810M_2 - 180M_1 + 9 = 630\,\bar{F}^4 m_4 + 2520\,\bar{F}^4 m_3 - 1260\,\bar{F}^3 m_3 + 3780\bar{F}^4 m_2 - 3780\,\bar{F}^3 m_2 + 810\,\bar{F}^2 m_2 + 630\bar{F}^4 - 1260\,\bar{F}^3 + 810\,\bar{F}^2 - 180\,\bar{F} + 9 \tag{19}$$
$$\cdots, \tag{20}$$

where of course $M_1 = \bar{F}$. We now see that there are three equivalent complete descriptions of the probability distribution function. The first one is in terms of binned PDF parameters B_i, the second one is in terms of either moments M_n or central normalized moments m_n, and the third one is in terms of coefficients of Legendre polynomials a_ℓ, which are completely given by the moments and allow one to "reconstruct" the actual PDF. Although the above equations might look terrifying, we note that these are trivially generated algorithmically to an arbitrary order.

We note that from the observational perspective, using moments or a_ℓ coefficients has a distinct advantage in that it is clear how the noise and $\bar{F}$ uncertainty enter the measurement. With respect to noise, the measurement of the i-th coefficient requires one to measure the noise-subtracted i-th moment. For a purely Gaussian noise, this is trivial, but any non-Gaussianity will contaminate $i > 2$ measurements, probably progressively so. Therefore, in the presence of noise, it is unlikely that one can measure, with very high precision more than a few first coefficients a_ℓ. Secondly, any uncertainty in $\bar{F}$ can be propagated in a fully understood manner into the covariance matrix for the final measurement, since we know exactly how it enters the measurement of the polynomial coefficients.

Finally, this method makes the complementarity with power spectrum calculations easier to understand. The power-spectrum is quadratic in the flux field data and hence the a_2 coefficient (or equivalently the second moments), as a function of the smoothing scale, are completely determined by the measurement of the power spectrum and the mean flux. The measurement of a_3 as a function of smoothing scale is akin to a reduced bispectrum, etc.

III. DEMONSTRATION ON SIMULATIONS

To demonstrate this method, we use the full hydrodynamic Gadget-3 simulations [18], evolved to redshift 2, with a WMAP7 cosmology, where $\Omega_{\rm m} = 0.275$, $\Omega_\Lambda = 0.725$, $\Omega_{\rm b} = 0.046$, $h_0 = 0.702$, $\sigma_8 = 0.816$, and $n_{\rm s} = 0.96$. The box size evolved is 80 Mpc/h, with $N = 2 \times 512^3$ for the number of gas and dark matter particles, and a Haardt and Madau UV background [19]. The simple QUICKLYA option is used for star formation with no feedback. We have simulated lines of sight on a 512×512 matrix on 1024 pixel-long skewers. We ignore the fact that in real data the skewers do not come as a perfect closely-packed grid in this paper's simplified treatment. In order to calculate the covariance matrix for the flux PDF and the subsequent method covariance matrices, we divide our flux field from the simulation

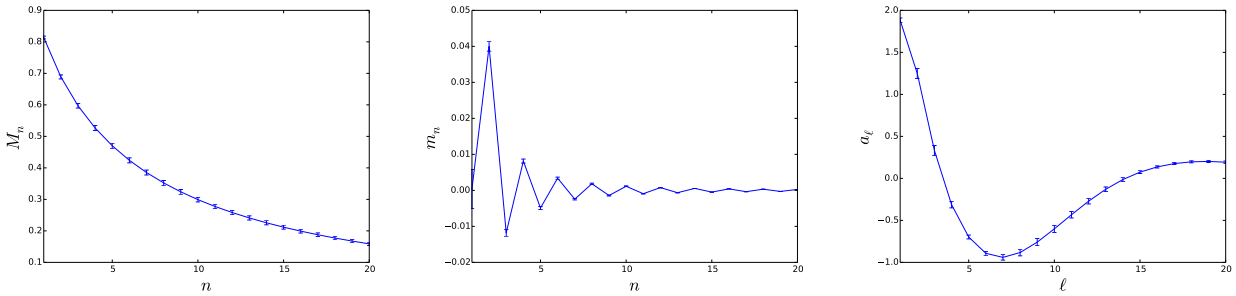

FIG. 2. Values of M_n in the left panel, m_n in the center, and a_ℓ in the right, at redshift 2, after smoothing the flux field with a smoothing scale of 1 Mpc/h in the line-of-sight direction.

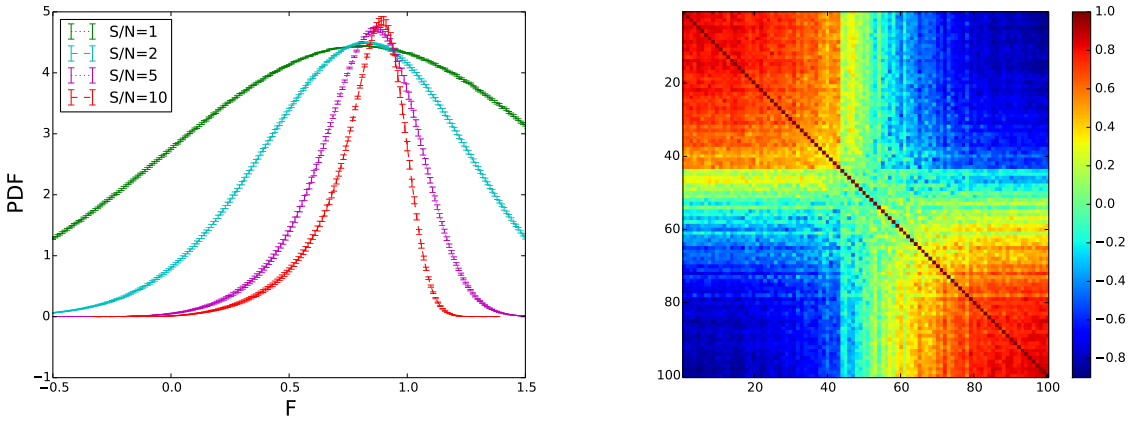

FIG. 3. PDF in left panel at redshift 2, after smoothing the flux field with a smoothing scale of 1 Mpc/h in the line-of-sight direction, and adding Gaussian noise for a signal-to-noise ratio (SNR) of 1 (green dotted line), 2 (cyan dashed line), 5 (magenta dotted line), and 10 (red dashed line). The covariance matrix for the corresponding B_i values for the SNR=1 is pictured in the right panel.

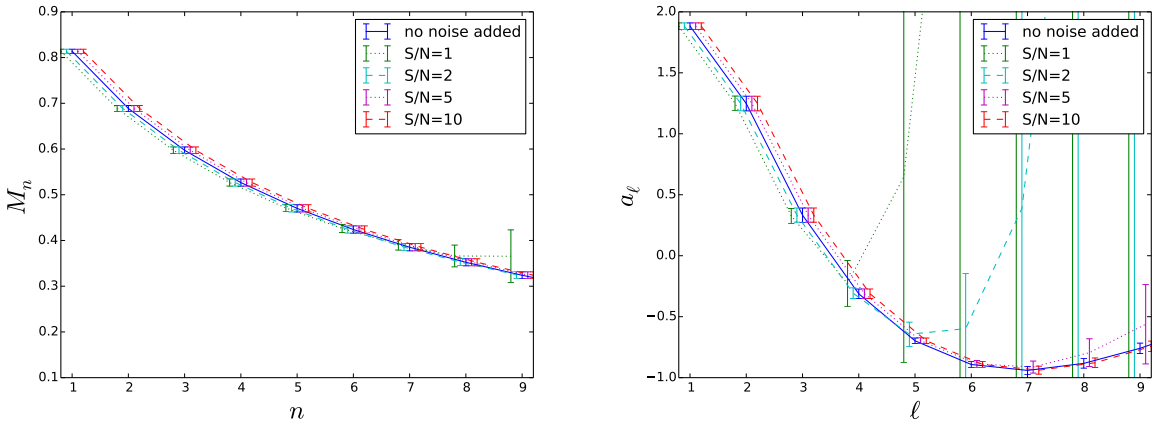

FIG. 4. Values of M_n in left panel and the reconstructed Legendre polynomial coefficients a_ℓ in the right panel, at redshift 2, after smoothing the flux field with a smoothing scale of 1 Mpc/h in the line-of-sight direction, and adding Gaussian noise for a signal-to-noise ratio of 1 (green dotted line), 2 (cyan dashed line), 5 (magenta dotted line), 10 (red dashed line). The no noise added line is represented as a blue continuous line. The lines are offset horizontally to better visualize the change in error bars.

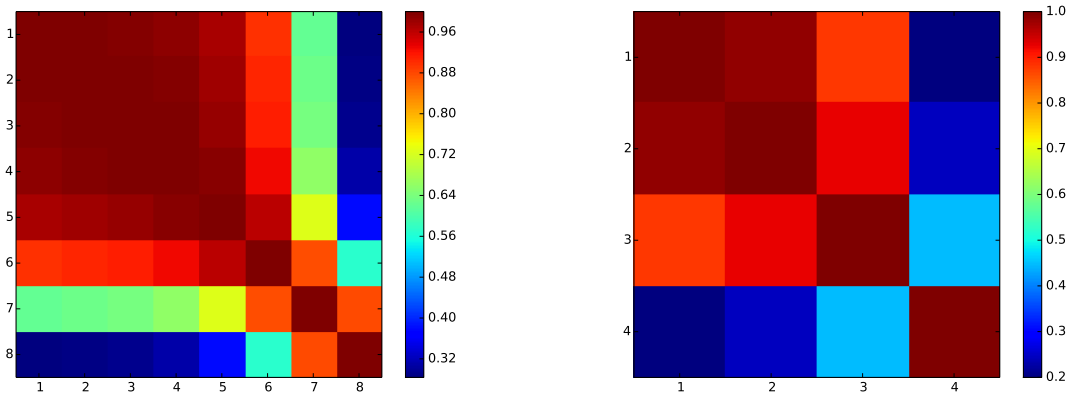

FIG. 5. Values of the reconstructed M_n covariance matrix in the left panel, and the reconstructed Legendre polynomial coefficients a_l covariance matrix in the right panel, both for a signal-to-noise ratio of 1 (represented as green dotted line in Figure 4).

into 64 cubes, and apply the bootstrap with replacement method for the error estimation with 1000 for the number of resamples. We do not rescale the mean flux in the simulations.

In this demonstration we will consider a rough equivalent of the BOSS experiment [20] and thus we first smooth the data on the scale of $1h$/Mpc in the radial direction to simulate the equivalent spectroscopic resolution. Figures 1 and 2 show the intrinsic flux PDF described using the four methods described above. We also plot the noise-less covariance matrix for the binned PDF description.

Next we add varying amount of noise to the data. Figure 3 shows the smoothed binned PDF, where we did not attempt to reconstruct the input PDF. The effect of noise is to splatter values of flux beyond the physically allowed range $0-1$ and demonstrates that a full forward-modeling is required to reconstruct the input flux PDF.

Finally, we calculate moments M_i by measuring raw moments in the data and then subtracting the noise contribution:

$$\tilde{M}_i = \frac{1}{N_{\rm points}} \sum_k F_k^i - N_i, \tag{21}$$

where $N_2 = \sigma^2$, $N_3 = 3\bar{F}\sigma^2$, $N_4 = 6\tilde{M}_2\sigma^2 + 3\sigma^4$, etc. with σ^2 being the variance of the error. This procedure can be trivially generalized to real data with varying noise, etc. This allows us to reconstruct values of a_ℓ and estimate the uncertainty. Since the coefficients a_ℓ are linear in M_i, our estimates for a_ℓ are unbiased. The results of this exercise are plotted in the Figure 4. We see that the addition of noise degrades measurements as expected. However, the effect is considerably more dramatic for the a_ℓ parameterization than it is for moments. For moments we see a slow increase in the uncertainties with errors on M_9 increasing markedly at low S/N but barely perceptible in others. On the other hand for a_ℓ coefficients, we note a noise-level dependent "wall" in ℓ: for SNR around 1, there is virtually no information at $\ell > 4$ and for SNR around 2, the same is true for $\ell > 6$. In other words, the transformation is very successful at compressing the information content into a few well-measured numbers.

In Figure 5 we show the covariance matrix for moments and Legendre polynomial coefficients for SNR~ 1. We see that well-determined moments are heavily correlated, but that the poorly determined ones are virtually uncorrelated. The correlation in the low ℓ modes most likely comes from sample variance which dominates their determination.

Finally, in Figure 6, we show the reconstructed PDF against the input PDF for the most likely solution. This is a sanity check. We see that SNR ~ 10 "reconstructs" the true PDF very well, but that low SNR data cannot resolve the peak. As we argued above, this information is truly lost.

IV. CONCLUSIONS

The properties of a random field are completely determined by the full set of n-point correlators. Any derived quantity such as PDF can in principle be derived from them.

In this paper we have made the link explicit for the Lyman-α forest flux, or any other field, for which the values of the field are limited to be in the finite range. We have shown that the first n moments of the field uniquely determined

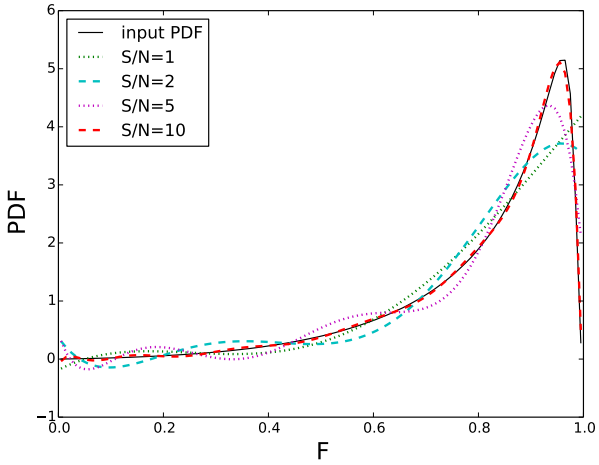

FIG. 6. Values of original and reconstructed (from legendre polynomials after subtracting noise) B_i at redshift 2, after smoothing the flux field with a smoothing scale of 1 Mpc/h in the line-of-sight direction. The color scheme used is the same as in Figure 4. The following legendre coefficients were used for each S/N line: coefficients 0-4 for the S/N=1 reconstruction, 0-5 for the S/N=2 reconstruction, 0-7 for the S/N=5 reconstruction, and 0-12 for the S/N=10 reconstruction.

the first n a_ℓ coefficients in the Legendre polynomial expansion of the PDF and vice-versa.

Using a toy-example, we argue that instead of measuring PDF, one should measure the a_ℓ coefficients. There are three main reasons for this:

- In our toy example these coeffients are very good at sorting the information content available in the PDF into a few well determined numbers and an infinite number of very poorly determined numbers. The precise number of well-determined coefficients is given by the SNR of the available data.
- Our procedure provides a very clear path to measuring these quantities: a_ℓ coefficients can be determined from the moments of the field for which unbiased estimators in the presence of noise are trivially computed.
- Mean flux $\bar{F}$ is often undeterminable from real data and its effect must be marginalised out assuming a plausible prior. Since $\bar{F}$ is just the first moment of the field, this marginalization is considerably easier than in the case of fitting binned flux distribution function.
- If a_ℓ coefficients are measured at a number of smoothing scales, a considerable statistical information is contained in a 2D field $a_\ell(k_s)$ with k_s being the smoothing wavenumber. In particular, assuming $\bar{F}$ to be known, the $a_2(k_s)$ contains the same information as the 1D power spectrum.

Before this method can be put in practce, more work needs to be done. On the observational side, the effects of metal contamination and damped Lyman-α systems need to be understood. On the theoretical side, m ore work needs to be done to establish the relation between these coefficients and physical properties of the inter-galactic medium, such as its mean flux, temperature-density relation and such. We leave this for future work.

ACKNOWLEDGEMENTS

We would like to thank Nishikanta Khandai for providing the Gadget-3 hydrodynamic simulations.

[1] P. McDonald, J. Miralda-Escudé, M. Rauch, W. L. W. Sargent, T. A. Barlow, R. Cen, and J. P. Ostriker, *The Observed Probability Distribution Function, Power Spectrum, and Correlation Function of the Transmitted Flux in the Lyα Forest*, *Astrophys. J.* **543** (Nov., 2000) 1–23.

[2] M. Viel, G. D. Becker, J. S. Bolton, and M. G. Haehnelt, *Warm dark matter as a solution to the small scale crisis: New constraints from high redshift Lyman-α forest data*, *Phys. Rev. D* **88** (Aug., 2013) 043502, [arXiv:1306.2314].

[3] U. Seljak, A. Makarov, P. McDonald, and H. Trac, *Can Sterile Neutrinos Be the Dark Matter?*, *Physical Review Letters* **97** (Nov., 2006) 191303–+.

[4] N. Afshordi, P. McDonald, and D. N. Spergel, *Primordial Black Holes as Dark Matter: The Power Spectrum and Evaporation of Early Structures*, *ApJ* **594** (Sept., 2003) L71–L74.

[5] N. Palanque-Delabrouille, C. Yèche, J. Lesgourgues, G. Rossi, A. Borde, M. Viel, E. Aubourg, D. Kirkby, J.-M. LeGoff, J. Rich, N. Roe, N. P. Ross, D. P. Schneider, and D. Weinberg, *Constraint on neutrino masses from SDSS-III/BOSS Lyα forest and other cosmological probes*, *JCAP* **2** (Feb., 2015) 45, [arXiv:1410.7244].

[6] J. Lesgourgues, G. Marques-Tavares, and M. Schmaltz, *Evidence for dark matter interactions in cosmological precision data?*, *ArXiv e-prints* (July, 2015) [arXiv:1507.04351].

[7] U. Seljak, A. Slosar, and P. McDonald, *Cosmological parameters from combining the Lyman-α forest with CMB, galaxy clustering and SN constraints*, *Journal of Cosmology and Astro-Particle Physics* **10** (Oct., 2006) 14–+.

[8] C. Dvorkin, K. Blum, and M. Kamionkowski, *Constraining dark matter-baryon scattering with linear cosmology*, *Phys. Rev. D* **89** (Jan., 2014) 023519, [arXiv:1311.2937].

[9] N. G. Busca, T. Delubac, J. Rich, S. Bailey, A. Font-Ribera, D. Kirkby, J.-M. Le Goff, M. M. Pieri, A. Slosar, É. Aubourg, J. E. Bautista, D. Bizyaev, M. Blomqvist, A. S. Bolton, J. Bovy, H. Brewington, A. Borde, J. Brinkmann, B. Carithers, R. A. C. Croft, K. S. Dawson, G. Ebelke, D. J. Eisenstein, J.-C. Hamilton, S. Ho, D. W. Hogg, K. Honscheid, K.-G. Lee, B. Lundgren, E. Malanushenko, V. Malanushenko, D. Margala, C. Maraston, K. Mehta, J. Miralda-Escudé, A. D. Myers, R. C. Nichol, P. Noterdaeme, M. D. Olmstead, D. Oravetz, N. Palanque-Delabrouille, K. Pan, I. Pâris, W. J. Percival, P. Petitjean, N. A. Roe, E. Rollinde, N. P. Ross, G. Rossi, D. J. Schlegel, D. P. Schneider, A. Shelden, E. S. Sheldon, A. Simmons, S. Snedden, J. L. Tinker, M. Viel, B. A. Weaver, D. H. Weinberg, M. White, C. Yèche, and D. G. York, *Baryon acoustic oscillations in the Lyα forest of BOSS quasars*, *A&A* **552** (Apr., 2013) A96, [arXiv:1211.2616].

[10] A. Slosar, V. Iršič, D. Kirkby, S. Bailey, N. G. Busca, T. Delubac, J. Rich, É. Aubourg, J. E. Bautista, V. Bhardwaj, M. Blomqvist, A. S. Bolton, J. Bovy, J. Brownstein, B. Carithers, R. A. C. Croft, K. S. Dawson, A. Font-Ribera, J.-M. Le Goff, S. Ho, K. Honscheid, K.-G. Lee, D. Margala, P. McDonald, B. Medolin, J. Miralda-Escudé, A. D. Myers, R. C. Nichol, P. Noterdaeme, N. Palanque-Delabrouille, I. Pâris, P. Petitjean, M. M. Pieri, Y. Piškur, N. A. Roe, N. P. Ross, G. Rossi, D. J. Schlegel, D. P. Schneider, N. Suzuki, E. S. Sheldon, U. Seljak, M. Viel, D. H. Weinberg, and C. Yèche, *Measurement of baryon acoustic oscillations in the Lyman-α forest fluctuations in BOSS data release 9*, *JCAP* **4** (Apr., 2013) 26, [arXiv:1301.3459].

[11] T. Delubac, J. E. Bautista, N. G. Busca, J. Rich, D. Kirkby, S. Bailey, A. Font-Ribera, A. Slosar, K.-G. Lee, M. M. Pieri, J.-C. Hamilton, É. Aubourg, M. Blomqvist, J. Bovy, J. Brinkmann, W. Carithers, K. S. Dawson, D. J. Eisenstein, S. G. A. Gontcho, J.-P. Kneib, J.-M. Le Goff, D. Margala, J. Miralda-Escudé, A. D. Myers, R. C. Nichol, P. Noterdaeme, R. O'Connell, M. D. Olmstead, N. Palanque-Delabrouille, I. Pâris, P. Petitjean, N. P. Ross, G. Rossi, D. J. Schlegel, D. P. Schneider, D. H. Weinberg, C. Yèche, and D. G. York, *Baryon acoustic oscillations in the Lyα forest of BOSS DR11 quasars*, *A&A* **574** (Feb., 2015) A59, [arXiv:1404.1801].

[12] E. B. Jenkins and J. P. Ostriker, *Lyman-alpha depression of the continuum from high-redshift quasars - A new technique applied in search of the Gunn-Peterson effect*, *Astrophys. J.* **376** (July, 1991) 33–42.

[13] J. S. Bolton, M. Viel, T.-S. Kim, M. G. Haehnelt, and R. F. Carswell, *Possible evidence for an inverted temperature-density relation in the intergalactic medium from the flux distribution of the Lyα forest*, *MNRAS* **386** (May, 2008) 1131–1144, [arXiv:0711.2064].

[14] M. Viel, J. S. Bolton, and M. G. Haehnelt, *Cosmological and astrophysical constraints from the Lyman α forest flux probability distribution function*, *MNRAS* **399** (Oct., 2009) L39–L43, [arXiv:0907.2927].

[15] K.-G. Lee, J. F. Hennawi, D. N. Spergel, D. H. Weinberg, D. W. Hogg, M. Viel, J. S. Bolton, S. Bailey, M. M. Pieri, W. Carithers, D. J. Schlegel, B. Lundgren, N. Palanque-Delabrouille, N. Suzuki, D. P. Schneider, and C. Yèche, *IGM Constraints from the SDSS-III/BOSS DR9 Lyα Forest Transmission Probability Distribution Function*, *Astrophys. J.* **799** (Feb., 2015) 196, [arXiv:1405.1072].

[16] A. Lidz, K. Heitmann, L. Hui, S. Habib, M. Rauch, and W. L. W. Sargent, *Tightening Constraints from the Lyα Forest with the Flux Probability Distribution Function*, *Astrophys. J.* **638** (Feb., 2006) 27–44, [astro-ph/0505138].

[17] R. Mandelbaum, P. McDonald, U. Seljak, and R. Cen, *Precision cosmology from the Lyman-α forest: power spectrum and bispectrum*, *MNRAS* **344** (Sept., 2003) 776–788.

[18] V. Springel, *The cosmological simulation code GADGET-2*, *MNRAS* **364** (Dec., 2005) 1105–1134, [astro-ph/0505010].

[19] F. Haardt and P. Madau, *Radiative Transfer in a Clumpy Universe. II. The Ultraviolet Extragalactic Background*, *Astrophys. J.* **461** (Apr., 1996) 20–+.

[20] K. S. Dawson, D. J. Schlegel, C. P. Ahn, S. F. Anderson, É. Aubourg, S. Bailey, R. H. Barkhouser, J. E. Bautista, A. Beifiori, A. A. Berlind, V. Bhardwaj, D. Bizyaev, C. H. Blake, M. R. Blanton, M. Blomqvist, A. S. Bolton, A. Borde, J. Bovy, W. N. Brandt, H. Brewington, J. Brinkmann, P. J. Brown, J. R. Brownstein, K. Bundy, N. G. Busca, W. Carithers, A. R. Carnero, M. A. Carr, Y. Chen, J. Comparat, N. Connolly, F. Cope, R. A. C. Croft, A. J. Cuesta, L. N. da Costa, J. R. A. Davenport, T. Delubac, R. de Putter, S. Dhital, A. Ealet, G. L. Ebelke, D. J. Eisenstein, S. Escoffier, X. Fan, N. Filiz Ak, H. Finley, A. Font-Ribera, R. Génova-Santos, J. E. Gunn, H. Guo, D. Haggard, P. B. Hall, J.-C. Hamilton, B. Harris, D. W. Harris, S. Ho, D. W. Hogg, D. Holder, K. Honscheid, J. Huehnerhoff, B. Jordan, W. P. Jordan, G. Kauffmann, E. A. Kazin, D. Kirkby, M. A. Klaene, J.-P. Kneib, J.-M. Le Goff, K.-G. Lee, D. C. Long, C. P. Loomis, B. Lundgren, R. H. Lupton, M. A. G. Maia, M. Makler, E. Malanushenko, V. Malanushenko, R. Mandelbaum, M. Manera, C. Maraston, D. Margala, K. L. Masters, C. K. McBride, P. McDonald, I. D. McGreer,

R. G. McMahon, O. Mena, J. Miralda-Escudé, A. D. Montero-Dorta, F. Montesano, D. Muna, A. D. Myers, T. Naugle, R. C. Nichol, P. Noterdaeme, S. E. Nuza, M. D. Olmstead, A. Oravetz, D. J. Oravetz, R. Owen, N. Padmanabhan, N. Palanque-Delabrouille, K. Pan, J. K. Parejko, I. Pâris, W. J. Percival, I. Pérez-Fournon, I. Pérez-Ràfols, P. Petitjean, R. Pfaffenberger, J. Pforr, M. M. Pieri, F. Prada, A. M. Price-Whelan, M. J. Raddick, R. Rebolo, J. Rich, G. T. Richards, C. M. Rockosi, N. A. Roe, A. J. Ross, N. P. Ross, G. Rossi, J. A. Rubiño-Martin, L. Samushia, A. G. Sánchez, C. Sayres, S. J. Schmidt, D. P. Schneider, C. G. Scóccola, H.-J. Seo, A. Shelden, E. Sheldon, Y. Shen, Y. Shu, A. Slosar, S. A. Smee, S. A. Snedden, F. Stauffer, O. Steele, M. A. Strauss, A. Streblyanska, N. Suzuki, M. E. C. Swanson, T. Tal, M. Tanaka, D. Thomas, J. L. Tinker, R. Tojeiro, C. A. Tremonti, M. Vargas Magaña, L. Verde, M. Viel, D. A. Wake, M. Watson, B. A. Weaver, D. H. Weinberg, B. J. Weiner, A. A. West, M. White, W. M. Wood-Vasey, C. Yeche, I. Zehavi, G.-B. Zhao, and Z. Zheng, *The Baryon Oscillation Spectroscopic Survey of SDSS-III*, *AJ* **145** (Jan., 2013) 10, [arXiv:1208.0022].